Available online at https://link.springer.com/journal/42241
http://www.jhydrodynamics.com
Journal of Hydrodynamics, 2019, 31(3): 455-463
https://doi.org/10.1007/s42241-019-0028-y

Objective Omega vortex identification method *

Jian-ming Liu[1, 2], Yi-sheng Gao[2], Yi-qian Wang[3], Chaoqun Liu[2]
1. *School of Mathematics and Statistics, Jiangsu Normal University, Xuzhou 221116, China*
2. *Department of Mathematics, University of Texas at Arlington, Arlington 76019, Texas, USA*
3. *School of Aerospace Engineering, Tsinghua University, Beijing 100084, China*

(Received February 24, 2019, Revised February 25, 2019, Accepted March 2, 2019, Published online March 14, 2019)

Abstract: A new vortex identification method (Liu et al. 2016) was proposed to represent the rotation relative strength and capture and visualize the vortices in our previous study. The basic idea of the Ω method is that a ratio of the vorticity squared over the summation of the vorticity squared and the deformation squared should be used to measure the relative rotation strength. However, the vorticity tensor norm is not objective. Thus, a moving observer will observe different vortex structures in a moving reference frame, which will make confusions about the real vortex structures. In the present study, by the definitions of the net spin tensor and the net vorticity vector, an objective Ω vortex identification method is presented with examples to verify that the vortex structures retain in a moving reference frame.

Key words: Vortex identification, the Ω method, objectivity, turbulence visualization, turbulence

Introduction

The turbulence is the most challenging and complex flow phenomenon in the fluid mechanics. The turbulent flow is composed of vortices, and without vortices, there will be no turbulence. The formation and the evolution of vortices determine the formation and the development of the turbulence. Therefore, the study of the vortex has a great significance in the fluid mechanics. As an intuitive understanding, the vortex is the part of fluid rotating around a certain axis. However, until now, the fluid mechanics community still has not reached a consensus of an exact definition of the vortex. In the fluid mechanics research community, the flow visualization is a very important tool for the study of the vortex structure of the turbulence. In order to analyze the vortex structure and make the flow field classification, various vortex identification methods were proposed to visualize the coherent structure in the turbulent flow.

In the classical theory of the fluid mechanics, vortices are often thought of as regions of high vorticity. Thus, the vorticity threshold criterion was used to identify the vortices where the connected region has a vorticity value over a given threshold[1-2]. However, Robinson et al.[3-5] found that the vorticity of the local rotation in a turbulent boundary layer may not be large, and the correlation between the vortex and the vorticity is rather weak. Furthermore, a laminar boundary layer possesses a large vorticity, but there is clearly no rotational motion in the laminar boundary layer. Hence, the vorticity criterion cannot distinguish the rotational vortices and the non-rotational shear layer. And the criterion is also not objective[2]. These motivate various ideas about a vortex, and various vortex identification methods were proposed.

The current popular vortex identification methods are mainly derived from the velocity gradient tensors. These methods include the Q criterion method[6], the Δ criterion method[7], the λ_2 criterion method[8], and the λ_{ci} criterion method[9]. In the Q criterion method, a vortex area is defined where the vorticity is greater than the deformation. In the Δ criterion method, vortices are located in the flow region where the vorticity is sufficiently strong to cause the rate-of-strain tensor to be dominated by the spin tensor, i.e., the velocity gradient tensor has

* Project supported by the National Nature Science Foundation of China (Grant Nos. 91530325, 11702159).
Biography: Jian-ming Liu (1977-), Male, Ph. D., Associate Professor, E-mail: jmliu@jsnu.edu.cn
Corresponding author: Chaoqun Liu, E-mail: cliu@uta.edu

complex eigenvalues[7]. The λ_{ci} criterion is an extension of the Δ criterion, and the scale of the imaginary part of the velocity gradient tensor is used to indicate the intensity of the vortex[2, 9]. The vortex structures given by these methods strongly depend on the threshold and the threshold can be arbitrary. If the threshold is too large, the weak vortex structure would disappear; if the threshold is too small, the weak vortex structure can be captured, but the strong vortex structure will be seriously smeared. Recently, a new method called the Ω method was proposed by Liu et al.[10], which assumes that the vortex is a connected region where the vorticity overtakes the deformation. The basic idea of the Ω method is that a ratio of the vorticity squared over the summation of the vorticity squared and the deformation squared should be used to measure the rotation strength. Ω is a non-dimensional scalar from 0 to 1 and it can be used to capture both strong and weak vortices simultaneously. This method has a clear physical meaning that the vortex is located where the vorticity overtakes the deformation. In addition, the Ω method is not sensitive to the threshold change and a larger range of the threshold values can be used to identify the vortex structure. Due to its obvious advantages, this method has gained widespread attentions for the vortex identification in turbulence[11-15], and is called the third generation vortex identification method[16]. Detailed review and comparative studies of these vortex identification methods can be found in Refs. [2, 12-13, 16].

Although the above methods have played a significant role in the turbulence visualization and the theoretical research, these methods are not objective[2, 17], because the parameters derived from the velocity gradient tensor are related with the reference frame of the observer. Thus, a rotating observer in a moving reference frame will observe different vortex structures[2]. The vortex identification method should be independent of the observer to make the results objective. For an objective method, the rotational effects of the observer's reference frame should be eliminated. Currently, there are mainly three kinds of balance methods in literature[2]. Drouot proposed to use the rotation rate of the eigenvectors of the strain-rate tensor to offset the rotation effects caused by the change of the observer's reference frame[18]. Wedgewood derived a very complicated rigid vorticity tensor to comply with the objectivity[19]. Recently, Haller et al.[20] defined a spatially-averaged vorticity to balance the effect of the moving observer in identifying objective Lagrangian and Eulerian vortices. In this paper, we will use the spatially-averaged vorticity to define an objective Ω method. The detailed mathematical derivation process and numerical examples will be provided.

1. Omega vortex identification method

The velocity gradient tensor

$$\nabla \boldsymbol{u} = \begin{bmatrix} \frac{\partial u}{\partial x} & \frac{\partial u}{\partial y} & \frac{\partial u}{\partial z} \\ \frac{\partial v}{\partial x} & \frac{\partial v}{\partial y} & \frac{\partial v}{\partial z} \\ \frac{\partial w}{\partial x} & \frac{\partial w}{\partial y} & \frac{\partial w}{\partial z} \end{bmatrix} \tag{1}$$

can be uniquely divided into symmetric and anti-symmetric parts, which are

$$\nabla \boldsymbol{u} = \begin{bmatrix} \frac{\partial u}{\partial x} & \frac{1}{2}\left(\frac{\partial u}{\partial y}+\frac{\partial v}{\partial x}\right) & \frac{1}{2}\left(\frac{\partial u}{\partial z}+\frac{\partial w}{\partial x}\right) \\ \frac{1}{2}\left(\frac{\partial v}{\partial x}+\frac{\partial u}{\partial y}\right) & \frac{\partial v}{\partial y} & \frac{1}{2}\left(\frac{\partial v}{\partial z}+\frac{\partial w}{\partial y}\right) \\ \frac{1}{2}\left(\frac{\partial w}{\partial x}+\frac{\partial u}{\partial z}\right) & \frac{1}{2}\left(\frac{\partial w}{\partial y}+\frac{\partial v}{\partial z}\right) & \frac{\partial w}{\partial z} \end{bmatrix} +$$

$$\begin{bmatrix} 0 & \frac{1}{2}\left(\frac{\partial u}{\partial y}-\frac{\partial v}{\partial x}\right) & \frac{1}{2}\left(\frac{\partial u}{\partial z}-\frac{\partial w}{\partial x}\right) \\ \frac{1}{2}\left(\frac{\partial v}{\partial x}-\frac{\partial u}{\partial y}\right) & 0 & \frac{1}{2}\left(\frac{\partial v}{\partial z}-\frac{\partial w}{\partial y}\right) \\ \frac{1}{2}\left(\frac{\partial w}{\partial x}-\frac{\partial u}{\partial z}\right) & \frac{1}{2}\left(\frac{\partial w}{\partial y}-\frac{\partial v}{\partial z}\right) & 0 \end{bmatrix} =$$

$$\boldsymbol{A}+\boldsymbol{B} \tag{2}$$

where $\boldsymbol{A}$ is a symmetric rate-of-strain tensor, and $\boldsymbol{B}$ is an antisymmetric spin tensor.

In the Ω method[10-11], a scalar is used to represent the relative rotation level, and it is assumed that the vortex will appear at the domain with the norm of the spin tensor exceeding the norm of the symmetrical strain-rate tensor. When the scalar value approaches 1, the fluid is near rigid or in a pure rotation.

In the original Ω method, the scalar is defined by

$$\Omega = \frac{\|\boldsymbol{B}\|_F^2}{\|\boldsymbol{A}\|_F^2 + \|\boldsymbol{B}\|_F^2 + \varepsilon} \tag{3}$$

where $\|\bullet\|_F$ denotes the Frobenius norm, $\|\boldsymbol{A}\|_F^2 = \mathrm{tr}(\boldsymbol{A}^{\mathrm{T}}\boldsymbol{A}) = \sum_{i=1}^{3}\sum_{j=1}^{3}(A_{ij}^2)$, and ε is a small magnitude to prevent the divisor become zero. Although, the

small parameter ε is suggested to be $\varepsilon = 0.001(\|\boldsymbol{B}\|_F^2 - \|\boldsymbol{A}\|_F^2)_{\max}$ in our previous paper[11], it still needs to be adjusted for some special problems. Furthermore, to capture both strong and weak vortex structures simultaneously, $\Omega = 0.52$ is empirically suggested by many researchers [11,13-14], and the Ω method is not sensitive to the threshold. However, as a most popular vortex identification method, the Q criterion is case-related and sensitive to the threshold change.

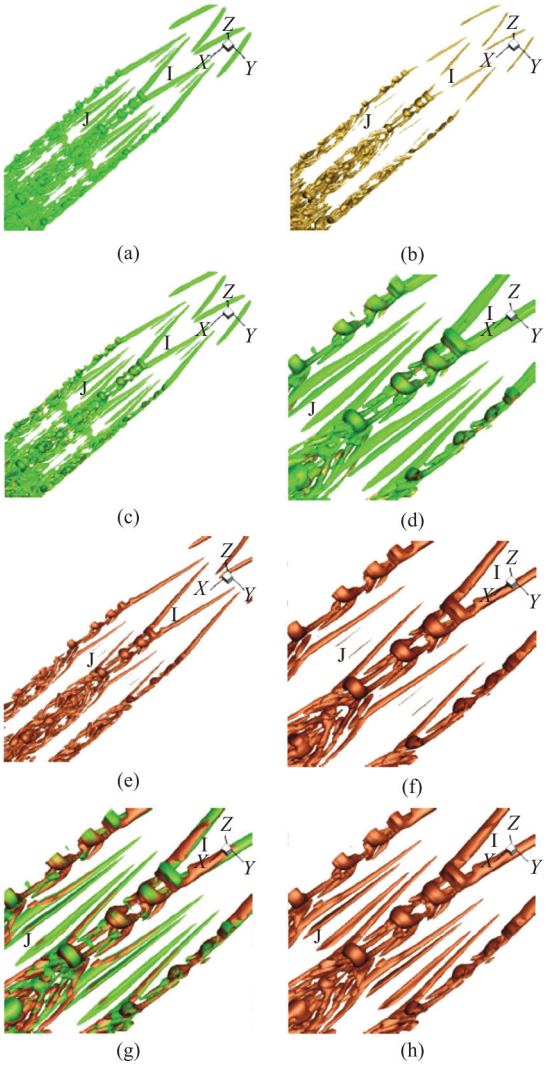

Fig. 1 (Color online) (a) Iso-surfaces with $\Omega = 0.52$, (b) Iso-surfaces with $Q = 0.01$, (c) Combination of (a) and (b), (d) Local view of (c), (e) Iso-surfaces with $\Omega = 0.52$, $Q = 0.005$, (f) Local view of (e), (g) Iso-surfaces with $\Omega = 0.52$, $Q = 0.0025$, (h) Iso-surfaces with $Q = 0.0025$

In order to support the conclusion, we use the data from a direct numerical simulation (DNS) of the boundary layer transition on a flat plate to demonstrate the use of the Ω method. The simulation is performed with about 60 million grid points and over 4×10^5 time steps at a free stream Mach number of 0.5 (see Ref. [21]). The iso-surfaces for the Ω method and the Q criterion are shown in Fig. 1. In these figures, the iso-surfaces with $\Omega = 0.52$ are shown in Fig. 1(a), and the iso-surfaces with $Q = 0.01$ are shown in Fig. 1(b), in which the leg of the hairpin vortex identified by the Q criterion is broken as shown at the point I. If we put Figs. 1(a), 1(b) together, we can easily conclude that the weak vortex is missed by $Q = 0.01$ at the point J (See Figs. 1(b), 1(c) and 1(d)). Although we can set Q to be a smaller value of 0.005, the streamwise weak vortex at the point J is still not clear (See Figs. 1(e), 1(f)). When $Q = 0.0025$, the weak vortex can be found (see Figs. 1(g), 1(h)). Therefore, whether the vortex is broken is determined by the threshold of the Q criterion but not the DNS data. This clearly shows that using the Q criterion to identify the vortex breaking is not suitable.

2. Objective Omega vortex identification method

For the vortex identification method to be objective, the identified results should be independent of the observer. In the present study, it is required that with the Ω vortex identification method, the same material region in the fluid should be located as a vortex regardless of the arbitrary translation or rotation of the observer[2]. However, the vorticity is not objective[2, 20]. Hence, the Ω method cannot be objective. If the criterion is not objective, the visualization results will depend on the rotating reference frame. In this section, we propose an objective Ω vortex identification method.

Objectivity requires the vortex identification criterion to be invariant under the following Euclidean frame change.

$$[x, y, z]^{\mathrm{T}} = \boldsymbol{Q}_r(t)[x^*, y^*, z^*]^{\mathrm{T}} + \boldsymbol{b}(t) \tag{4}$$

where x, y, z represent the coordinates in the original reference frame and x^*, y^*, z^* represent the coordinates in the new reference frame, and $\boldsymbol{Q}_r(t)$ is a rotation matrix with the orthogonal property, i.e., $\boldsymbol{Q}_r^{\mathrm{T}}\boldsymbol{Q}_r = \boldsymbol{Q}_r\boldsymbol{Q}_r^{\mathrm{T}} = \mathbf{I}$, and $\boldsymbol{b}(t)$ is a translation, and both are possibly time-dependent. If $\boldsymbol{Q}_r(t)$ is independent of time and $\boldsymbol{b}(t) = \boldsymbol{c}_1 t + \boldsymbol{c}_2$ with a static rotation and a constant-velocity translation, we call this special case a Galilean transformation. Due to the orthogonal invariance of the Frobenius norm, it is easy

to prove the original Ω method is Galilean invariant.

The velocity vector $\boldsymbol{u}^* = \left[u^*, v^*, w^*\right]^{\mathrm{T}}$ in the new reference frame can be written as

$$\boldsymbol{u}^* = \boldsymbol{Q}_r^{\mathrm{T}}(t)\boldsymbol{u} + \dot{\boldsymbol{Q}}_r^{\mathrm{T}}(t)[x, y, z]^{\mathrm{T}} - \frac{\mathrm{d}}{\mathrm{d}t}[\boldsymbol{Q}_r^{\mathrm{T}}(t)\boldsymbol{b}(t)] \tag{5}$$

where u, v, w represent the velocity components in the original reference frame, and $\dot{\boldsymbol{Q}}_r(t)$ is the derivative matrix. From Eq. (5), we can obtain the velocity gradient tensor in the new reference frame as

$$\nabla \boldsymbol{u}^* = \boldsymbol{Q}_r^{\mathrm{T}}(t)\nabla \boldsymbol{u}\boldsymbol{Q}_r(t) + \dot{\boldsymbol{Q}}_r^{\mathrm{T}}(t)\boldsymbol{Q}_r(t) \tag{6}$$

With the moving observer rotating as in Eq. (4), the antisymmetric spin tensor in the new reference frame can be formulated as

$$\boldsymbol{B}^* = \boldsymbol{Q}_r^{\mathrm{T}}(t)\boldsymbol{B}\boldsymbol{Q}_r(t) - \boldsymbol{Q}_r^{\mathrm{T}}(t)\dot{\boldsymbol{Q}}_r(t) \tag{7}$$

which explains why both the original Ω method and the popular Q criterion are not objective.

In order to design an objective Ω method, we firstly prove some mathematical lemmas.

Lemma 1: If $\boldsymbol{Q}_r(t) \in R^{3\times 3}$ is orthogonal, then

$$\dot{\boldsymbol{Q}}_r^{\mathrm{T}}(t)\boldsymbol{Q}_r(t) + \boldsymbol{Q}_r^{\mathrm{T}}(t)\dot{\boldsymbol{Q}}_r(t) = 0 \tag{8}$$

Proof. Since $\boldsymbol{Q}_r(t) \in R^{3\times 3}$ is orthogonal. So, we have

$$\boldsymbol{Q}_r^{\mathrm{T}}(t)\boldsymbol{Q}_r(t) = \mathbf{I} \tag{9}$$

Take derivative of Eq. (9), we have

$$\frac{\mathrm{d}}{\mathrm{d}t}[\boldsymbol{Q}_r^{\mathrm{T}}(t)\boldsymbol{Q}_r(t)] = 0 \tag{10}$$

Thus

$$\frac{\mathrm{d}}{\mathrm{d}t}[\boldsymbol{Q}_r^{\mathrm{T}}(t)\boldsymbol{Q}_r(t)] = \dot{\boldsymbol{Q}}_r^{\mathrm{T}}(t)\boldsymbol{Q}_r(t) + \boldsymbol{Q}_r^{\mathrm{T}}(t)\dot{\boldsymbol{Q}}_r(t) = 0$$

This completes the proof of Lemma 1.

Lemma 2: The tensor $\boldsymbol{B}^*$ in the new reference frame is antisymmetric.

Proof. For $\boldsymbol{B}^* = \boldsymbol{Q}_r^{\mathrm{T}}(t)\boldsymbol{B}\boldsymbol{Q}_r(t) - \boldsymbol{Q}_r^{\mathrm{T}}(t)\dot{\boldsymbol{Q}}_r(t)$, the antisymmetric property requires $\boldsymbol{B}^{*\mathrm{T}} = -\boldsymbol{B}^*$. Notice that

$$\boldsymbol{B}^{*\mathrm{T}} = [\boldsymbol{Q}_r^{\mathrm{T}}(t)\boldsymbol{B}\boldsymbol{Q}_r(t) - \boldsymbol{Q}_r^{\mathrm{T}}(t)\dot{\boldsymbol{Q}}_r(t)]^{\mathrm{T}} =$$

$$\boldsymbol{Q}_r^{\mathrm{T}}(t)\boldsymbol{B}^{\mathrm{T}}\boldsymbol{Q}_r(t) - \dot{\boldsymbol{Q}}_r^{\mathrm{T}}(t)\boldsymbol{Q}_r(t) \tag{11}$$

From Eq. (8)

$$\dot{\boldsymbol{Q}}_r^{\mathrm{T}}(t)\boldsymbol{Q}_r(t) = -\boldsymbol{Q}_r^{\mathrm{T}}(t)\dot{\boldsymbol{Q}}_r(t)$$

and notice that $\boldsymbol{B}^{\mathrm{T}} = -\boldsymbol{B}$, we have

$$\boldsymbol{B}^{*\mathrm{T}} = -\boldsymbol{Q}_r^{\mathrm{T}}(t)\boldsymbol{B}\boldsymbol{Q}_r(t) + \boldsymbol{Q}_r^{\mathrm{T}}(t)\dot{\boldsymbol{Q}}_r(t) = -\boldsymbol{B}^*$$

completing the proof of the Lemma 2.

Lemma 3[22]**: (Orthogonal Invariance)** If $\boldsymbol{C} \in R^{m\times n}$ is an any matrix, and the matrices $\boldsymbol{M} \in R^{m\times m}$ and $\boldsymbol{N} \in R^{n\times n}$ are orthogonal, then $\|\boldsymbol{MCN}\|_F = \|\boldsymbol{C}\|_F$.

Proof. The lemma follows from the orthogonal invariance of the vector 2-norm. In fact

$$\|\boldsymbol{MC}\|_F^2 = \sum_{j=1}^{n}\|\boldsymbol{MC}(:, j)\|_2^2 = \sum_{j=1}^{n}\|\boldsymbol{C}(:, j)\|_2^2 = \|\boldsymbol{C}\|_F^2$$

and so

$$\|\boldsymbol{M}(\boldsymbol{CN})\|_F^2 = \|\boldsymbol{CN}\|_F^2 = \|\boldsymbol{N}^{\mathrm{T}}\boldsymbol{C}^{\mathrm{T}}\|_F^2 = \|\boldsymbol{C}^{\mathrm{T}}\|_F^2 = \|\boldsymbol{C}\|_F^2$$

From Eqs. (6), (7), noticing Eq. (8), we can obtain the symmetric rate-of-strain tensor in the new reference frame that

$$\boldsymbol{A}^* = \nabla \boldsymbol{u}^* - \boldsymbol{B}^* = \boldsymbol{Q}_r^{\mathrm{T}}(t)\boldsymbol{A}\boldsymbol{Q}_r(t) \tag{12}$$

Hence the symmetric rate-of-strain tensor is objective. If we want the antisymmetric spin tensor to be objective, we must counteract the term $\boldsymbol{Q}_r^{\mathrm{T}}(t)\dot{\boldsymbol{Q}}_r(t)$ in Eq. (7). There are three methods in the literature for the objective treatment[2]. In the present study, we use the spatially-averaged vorticity proposed by Haller et al.[20] to design an objective Ω method. We recall that the vorticity $\boldsymbol{\omega} = \nabla \times \boldsymbol{u}$ The instantaneous spatial mean $\bar{\boldsymbol{\omega}}$ of the vorticity over $V(t)$, which is the whole volume of the fluid, is defined by

$$\bar{\boldsymbol{\omega}}(t) = \frac{1}{V(t)}\int_{V(t)} \boldsymbol{\omega}(x, y, z; t)\mathrm{d}V \tag{13}$$

From Eq. (13), we can obtain an antisymmetric tensor $\bar{\boldsymbol{B}}$ and

$$\bar{\boldsymbol{B}}\boldsymbol{e} = \frac{1}{2}\bar{\boldsymbol{\omega}} \times \boldsymbol{e}, \forall \boldsymbol{e} \in R^3 \tag{14}$$

In the new reference frame (4), the vorticity $\boldsymbol{\omega}$ will become

$$\boldsymbol{\omega}^* = \boldsymbol{Q}_r^{\mathrm{T}}(t)\boldsymbol{\omega} + \dot{\boldsymbol{q}}(t) \tag{15}$$

where the vector $\dot{\boldsymbol{q}}(t)$ satisfies the relation $\boldsymbol{Q}_r^{\mathrm{T}}(t) \cdot \dot{\boldsymbol{Q}}_r(t)\boldsymbol{e} = -(\dot{\boldsymbol{q}} \times \boldsymbol{e})/2$ for all $\boldsymbol{e} \in R^3$, and the spatially-averaged vorticity will be given by

$$\bar{\boldsymbol{\omega}}^* = \boldsymbol{Q}_r^{\mathrm{T}}(t)\bar{\boldsymbol{\omega}} + \dot{\boldsymbol{q}}(t) \tag{16}$$

with its corresponding antisymmetric tensor $\bar{\boldsymbol{B}}^*$, satisfying

$$\bar{\boldsymbol{B}}^*\boldsymbol{e} = \frac{\bar{\boldsymbol{\omega}}^* \times \boldsymbol{e}}{2} = \frac{[\boldsymbol{Q}_r^{\mathrm{T}}(t)\bar{\boldsymbol{\omega}} + \dot{\boldsymbol{q}}(t)] \times \boldsymbol{e}}{2} =$$

$$\frac{\boldsymbol{Q}_r^{\mathrm{T}}(t)\bar{\boldsymbol{\omega}} \times \boldsymbol{e}}{2} - \boldsymbol{Q}_r^{\mathrm{T}}(t)\dot{\boldsymbol{Q}}_r(t)\boldsymbol{e} \tag{17}$$

Hence, we can obtain

$$\bar{\boldsymbol{B}}^* = \boldsymbol{Q}_r^{\mathrm{T}}(t)\bar{\boldsymbol{B}}\boldsymbol{Q}_r(t) - \boldsymbol{Q}_r^{\mathrm{T}}(t)\dot{\boldsymbol{Q}}_r(t) \tag{18}$$

In fact, Eq. (18) can also be derived from Eq. (7). Then we give the definitions of the net spin tensor and the net vorticity vector as follows

$$\tilde{\boldsymbol{B}} = \boldsymbol{B} - \bar{\boldsymbol{B}}, \quad \tilde{\boldsymbol{\omega}} = \boldsymbol{\omega} - \bar{\boldsymbol{\omega}} \tag{19}$$

In the new reference frame (4), noticing Eqs. (7), (15)-(18), the corresponding net spin tensor and net vorticity vector are

$$\tilde{\boldsymbol{B}}^* = \boldsymbol{B}^* - \bar{\boldsymbol{B}}^* = \boldsymbol{Q}_r^{\mathrm{T}}(t)\tilde{\boldsymbol{B}}\boldsymbol{Q}_r(t),$$

$$\tilde{\boldsymbol{\omega}}^* = \boldsymbol{\omega}^* - \bar{\boldsymbol{\omega}}^* = \boldsymbol{Q}_r^{\mathrm{T}}(t)\tilde{\boldsymbol{\omega}} \tag{20}$$

respectively. From formula (20) and Lemma 3, we can conclude that the net spin tensor and the net vorticity vector are objective under the Frobenius norm, which leads to the following theorem.

Theorem 1: The new parameter for the objective Omega method can be defined by

$$\tilde{\Omega} = \frac{\left\|\tilde{\boldsymbol{B}}\right\|_F^2}{\left\|\boldsymbol{A}\right\|_F^2 + \left\|\tilde{\boldsymbol{B}}\right\|_F^2 + \varepsilon} \tag{21}$$

where $\tilde{\boldsymbol{B}}$ is the net spin tensor defined by Eqs. (19), $\boldsymbol{A}$ is the symmetric rate-of-strain tensor defined in Eq. (2), and ε is a small magnitude to prevent the divisor to become zero.

As a direct corollary, the objective $\tilde{Q}$ criterion can be defined by $\tilde{Q} = (\left\|\tilde{\boldsymbol{B}}\right\|_F^2 - \left\|\boldsymbol{A}\right\|_F^2)/2$.

3. Numerical examples

In the following, four examples are presented to implement the objective Ω method. All examples involve variable-time rotating and translation frames. The different iso-surfaces of the vortex structures indicate the importance of the objectivity of the vortex identification methods.

3.1 *Burgers vortex*

As the first example, the Burgers vortex is used to test the objectivity of the present method. The Burgers vortex generally is a stationary and self-similar flow, as an exact steady solution to the Navier-Stokes equations, and is often used to describe the vortex stretching mechanism or as a simplified model of tornado[23]. The velocity components of the Burgers vortex are generally formulated in cylindrical coordinates by

$$u_r = -\alpha r, \quad u_\theta = \frac{\Gamma}{2\pi r}\left[1 - \exp\left(-\frac{\alpha r^2}{2\nu}\right)\right], \quad u_z = 2\alpha z \tag{22}$$

where $\alpha > 0$, Γ is a constant. In the present study, we take $\alpha = 1$, $\nu = 0.02$ and $\Gamma = 5$

To study a general objectivity of the present method, the variable-time rotation matrix $\boldsymbol{Q}_r(t)$ with three basic rotations around three coordinate axes is considered.

$$\boldsymbol{Q}_r(t) = \boldsymbol{Q}_{rx}(\gamma_1 t)\boldsymbol{Q}_{ry}(\gamma_2 t)\boldsymbol{Q}_{rz}(\gamma_3 t) =$$

$$\begin{bmatrix} 1 & 0 & 0 \\ 0 & \cos\gamma_1 t & \sin\gamma_1 t \\ 0 & -\sin\gamma_1 t & \cos\gamma_1 t \end{bmatrix}\begin{bmatrix} \cos\gamma_2 t & 0 & -\sin\gamma_2 t \\ 0 & 1 & 0 \\ \sin\gamma_2 t & 0 & \cos\gamma_2 t \end{bmatrix} \cdot$$

$$\begin{bmatrix} \cos\gamma_3 t & \sin\gamma_3 t & 0 \\ -\sin\gamma_3 t & \cos\gamma_3 t & 0 \\ 0 & 0 & 1 \end{bmatrix} \tag{23}$$

where γ_1, γ_2 and γ_3 are the corresponding rotational angular speeds around the coordinate axes.

In this study we randomly choose $\gamma_1 = 0.35$, $\gamma_2 = 2.25$ and $\gamma_3 = 1.50$ In addition, the translation $\boldsymbol{b}(t) = \left[1, t^2, 0.5\right]^{\mathrm{T}}$ is considered between the new reference frame (at time $t = 0.5$) and the original reference frame.

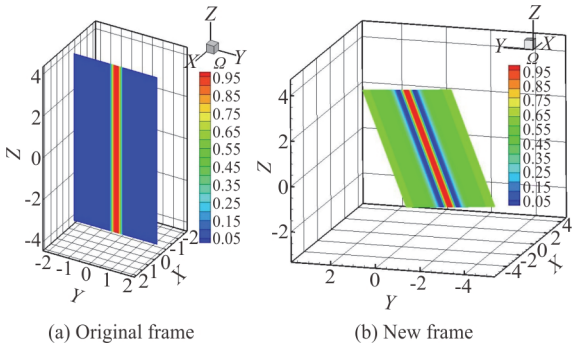

Fig. 2 (Color online) Non-objective Ω of Burgers vortex

The contours of Ω in different reference frames are shown in Fig. 2. It is clear to see that, with the variable-time rotating and spatial translation frames, the original Ω method cannot retain the vortex structure correctly and the value of Ω changes greatly, and the areas without vortices are mistakenly identified as the vortex areas. As a comparation, the contours of $\tilde{\Omega}$ in different variable-time reference frames are displayed in Fig. 3. We can easily find that the present objective $\tilde{\Omega}$ method can retain the vortex structure and retain the value of $\tilde{\Omega}$.

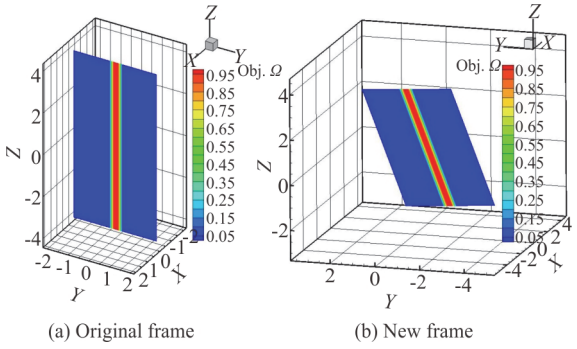

Fig. 3 (Color online) Objective Ω of Burgers vortex

To further quantify the objectivity of the present method, we calculate the original Ω and the objective $\tilde{\Omega}$ at $A(-0.13141, 0.35294, 3.96553)$ in the original reference frame and its corresponding point $A^*(2.25, 1.41, -2.50)$ in the new reference frame. From our calculation, at the original point A, $\Omega = 0.013872$, $\tilde{\Omega} = 8.06 \times 10^{-3}$, and at new reference point A^*, $\Omega = 0.211281$, $\tilde{\Omega} = 8.06 \times 10^{-3}$. Hence the original Ω method is not objective, and the new version is objective and can retain the value of $\tilde{\Omega}$ between the original and new reference frames.

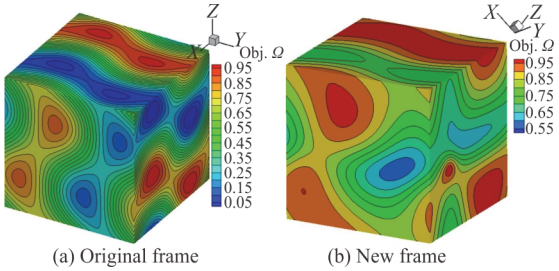

Fig. 4 (Color online) Non-objective Ω of ABC flow

3.2 *Unsteady ABC-type flow*

Next, as an unstable solution of the Euler equation, the ABC flow with high-frequency instabilities under perturbation is studied by the Ω method. In this special case, the unsteady velocity field is

$$u(x, y, z; t) = A(t)\sin z + C\cos y,$$

$$v(x, y, z; t) = B\sin x + A(t)\cos z,$$

$$w(x, y, z; t) = C\sin y + B\cos x \tag{24}$$

In Eq. (24), $A(t) = A_0 + (1 - \mathrm{e}^{-qt})\sin \omega t$ represents the effect of a growing and saturating unstable mode[24]. Here, $A_0 = \sqrt{3}$, $q = 0.1$, $\omega = 2\pi$, $B = \sqrt{2}$ and $C = 1$ We also give the vortex contours in the different variable-time moving reference frames. In this case, we use the same transformation formulated by Eq. (23). The rotational angular speeds γ_1, γ_2, γ_3 and translation vector $\boldsymbol{b}(t)$ are the same as the settings in the example of the Burgers vortex.

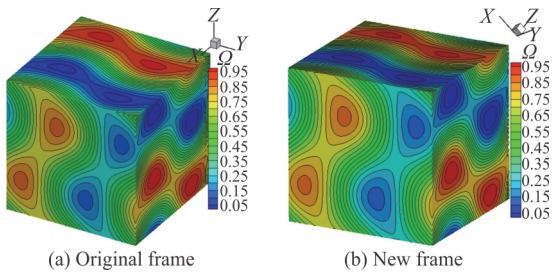

Fig. 5 (Color online) Objective Ω of ABC flow

The contours of the original Ω in different reference frames are shown in Fig. 4. The original non-objective Ω method obviously can not identify

the vortex structure, and the vortex visualization is changes greatly, as can be seen from the right figure in Fig. 4. However, the objective Ω method can retain the vortex structure with the impact of the variable-time reference frame (see Fig. 5). The conclusion also can be observed by the iso-surfaces as shown in Fig. 6. With the non-objective $\Omega = 0.65$, most of the vortex structures disappear. However, the objective $\tilde{\Omega}$ keeps the vortex structure.

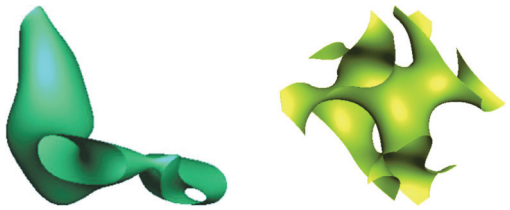

(a) Non-objective Ω (b) Objective Ω

Fig. 6 (Color online) The iso-surfaces at $\Omega = 0.65$

3.3 *Objective vortex structures in the flow from micro-vortex generator (MVG)*

In order to show the importance of the objectivity, the data from an implicitly implemented LES (ILES) method for a supersonic flow with the flow control by the micro-vortex generator (MVG) are studied, where the shock wave and the boundary layer interaction (SWBLI) are calculated at Mach number 2.5. The numerical simulation for this special case is performed by an optimized weighted essentially non-oscillatory (WENO) scheme on a body-fitted structural grid system with about 40 million points. The computational details can be found in the paper[25].

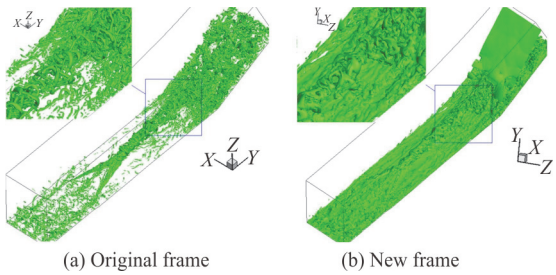

(a) Original frame (b) New frame

Fig. 7 (Color online) The iso-surfaces by the non-objective $\Omega(=0.52)$ method

We choose the variable-time reference frame (23) with the same settings as before. For this special problem, the Ω method can easily capture a variety of strong and weak vortices, in which the iso-surfaces with non-objective $\Omega(=0.52)$ method are shown in Fig. 7(a). With Eq. (23), the reference frame has non-zero speed and acceleration. Using the non-objective Ω method, the flow field will be completely polluted (see Fig. 7(b)). Hence, the non-objective method cannot be used in the variable-time reference frame. The result obtained by the objective $\tilde{\Omega}$ method is shown in Fig. 8. Except for some computer rounding errors, the vortices in the different reference frames are almost the same.

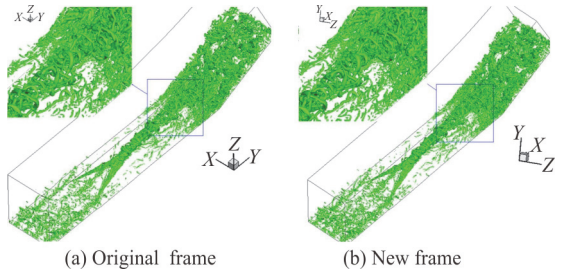

(a) Original frame (b) New frame

Fig. 8 (Color online) The iso-surfaces by the objective $\Omega(=0.52)$ method

3.4 *Rotating machinery*

In the field of a rotating machinery, including the rotor and the wind turbine, the objectivity of the vortex is an important issue. The vortex structure should not be varied by the observer's position. In this special example, we consider a rotor with the blade tip Mach number of 0.44 at a subsonic hovering state. The calculation is done by an in-house code with a second order finite volume hybrid Cartesian grid method[26]. Here the structural body-fitted grid is used in the near-body domain of the two rotor blades and the adaptive Cartesian grid is used in the off-body domain. Due to the accuracy limitation of the second-order finite volume method, the tip vortex identified by the numerical method is very weak and therefore the original suggestion of ε for the Ω method in paper[11] is not suitable. According to our research, for the very weak vortices, the value of ε should also be adjusted correspondingly. In this special example, we set $\varepsilon = 2\times10^{-5}(\|\boldsymbol{B}\|_F^2 - \|\boldsymbol{A}\|_F^2)_{\max}$. For the variable-time rotation matrix $\boldsymbol{Q}_r(t)$, we choose $\gamma_1 = 0.035$, $\gamma_2 = -0.0125$ and $\gamma_3 = -0.005$. In addition, a new time-variable translation $\boldsymbol{b}(t) = [0.05t^3, 0.02t^2, 0.035t]^{\mathrm{T}}$ is considered between the new reference frame (at time $t = 0.5$) and the original reference frame. Although the rotational angular speed for this case is small, in the moving reference frame, the vortex structures are completely contaminated as shown on the right of Fig. 9. Hence, for a moving observer, the non-objective Ω method is not suitable. Using the present objective Ω vortex identification method, one can see that, from Fig. 10, the vortex structures in the moving reference frame are almost identical for a moving observer.

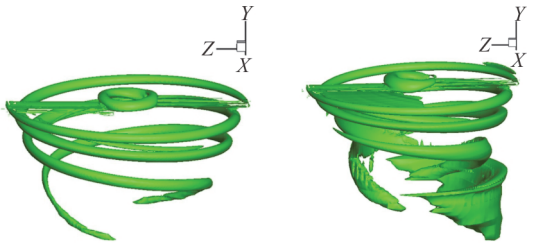

(a) Original frame (b) New frame

Fig. 9 (Color online) Original non-objective Ω of rotor flow

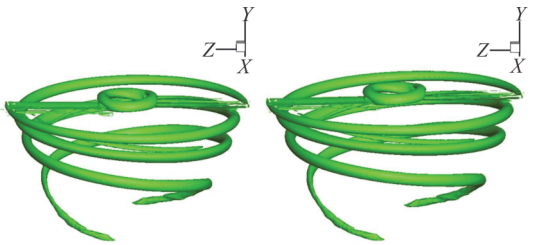

(a) Original frame (b) New frame

Fig. 10 (Color online) Objective Ω of rotor flow

4. Conclusion

In this paper, an objective Ω method is derived in detail. The developed method is carefully checked for some three-dimensional flow fields. Two analytical and explicit vortex solutions of the Navier-Stokes equations and the Euler equation are selected to demonstrate and test the objective Ω method. In addition, the data from the ILES is visualized by the non-objective and objective Ω methods in different reference frames. Furthermore, the visualization of a rotor flow is presented to show the importance of the objectivity of the vortex identification methods for a moving observer and the rotational machinery. The results show that, if the transformations of a spatial rotation and a translation are both time related, the original Ω method is not objective and will pollute the flow visualization. However, the new $\tilde{\Omega}$ method is objective and will not be contaminated by the rotating observers, as is verified by several practical examples.

Acknowledgments

This work was supported by the Natural Science Foundation of the Jiangsu Higher Education Institutions of China (Grant Nos.18KJA110001), the Visiting Scholar Scholarship of the China Scholarship Council (Grant No. 201808320079), and the China Post-Doctoral Science Foundation (Grant No. 2017M610876). This work is partly accomplished by using code DNSUTA and LESUTA developed by Dr. Chaoqun Liu at the University of Texas at Arlington, and by using code CABA developed by Dr. Ning Zhao at Nanjing University of Aeronautics and Astronautics.

References

[1] Epps B. P., Alvarado P. V., Youcef-Toumi K. et al. Swimming Performance of a biomimetic compliant fish-like robot [J]. *Experiments in Fluids*, 2009, 47(6): 927-939.

[2] Epps B. P. Review of vortex identification methods [C]. *55th AIAA Aerospace Sciences Meeting*, Grapevine, Texas, USA, 2017.

[3] Robinson S. K. A review of vortex structures and associated coherent motions in turbulent boundary layers. In structure of turbulence and drag reduction [M]. Berlin, Germany: Springer, 1990, 23-50.

[4] Robinson S. K., Kline S. J., Spalart P. R. A review of quasi-coherent structures in a numerically simulated turbulent boundary layer [R]. *NASA Technical Memorandum*, 1989, 102191.

[5] Liu C., Cai X. New theory on turbulence generation and structure–DNS and experiment [J]. *Science China Physics, Mechanics and Astronomy*, 2017, 60(8): 084731.

[6] Hunt J. C. R., Wray A. A., Moin P. Eddies, streams, and convergence zones in turbulent flows [C]. *Proceedings of the Summer Program. Center for Turbulence Research*, Stanford, USA, 1988, 193-208.

[7] Chong M. S., Perry A. E., Cantwell B. J. A general classification of three-dimensional flow fields [J]. *Physics of Fluids*, 1990, 2(5): 765-777.

[8] Jeong J., Hussain F. On the identification of a vortex [J]. *Journal of Fluid Mechanics*, 1995, 285: 69-94.

[9] Zhou J., Adrian, R. J., Balachandar S. et al. Mechanisms for generating coherent packets of hairpin vortices in channel flow [J]. *Journal of Fluid Mechanics*, 1999, 387(5): 353-396.

[10] Liu C., Wang Y. Q., Yang Y. et al. New omega vortex iden- tification method [J]. *Science China Physics, Mechanics and Astronomy*, 2016, 59(8): 684711.

[11] Dong X. Q., Wang Y. R., Chen X. P. et al. Determination of epsilon for Omega vortex identification method [J]. *Journal of Hydrodynamics,* 2018, 30(4): 541-548.

[12] Zhang Y., Liu K., Xian H. et al. A review of methods for vortex identification in hydroturbines [J]. *Renewable and Sustainable Energy Reviews*, 2018, 81: 1269-1285.

[13] Zhang Y. N., Qiu X., Chen F. P. et al. A selected review of vortex identification methods with applications [J]. *Journal of Hydrodynamics*, 2018, 30(5): 767-779.

[14] Zhang Y. N., Liu K. H., Li J. W. et al. Analysis of the vortices in the inner flow of reversible pump turbine with the new omega vortex identification method [J]. *Journal of Hydrodynamics*, 2018, 30(3): 463-469.

[15] Kareem W. A. Anisotropic complex diffusion filtering for comparison of the vortex identification methods in homogeneous turbulence [J]. *International Journal of Mechanical Sciences*, 2017, 134: 291-305.

[16] Liu C., Gao Y., Dong X. et al. Third generation of vortex identification methods: Omega and Liutex/Rortex based systems [J]. *Journal of Hydrodynamics*, 2019, 31(2): 205-223.

[17] Martins R. S., Pereira A. S., Mompean G. et al. An objective perspective for classic flow classification criteria [J].

Comptes Rendus Mecanique, 2016, 344(1): 52-59.
[18] Drouot R. Définition d'un transport associé à un modèle de fluide du deuxième ordre. Comparaison de diverses lois de comportement [J]. *Comptesrendus de l'Académie des Sciences, Série A*, 1976, 282: 923-926(in French).
[19] Wedgewood L. E. An objective rotation tensor applied to non-Newtonian fluid mechanics [J]. *Rheologica Acta*, 1999, 38(2): 91-99.
[20] Haller G., Hadjighasem A., Farazmand M. et al. Defining coherent vortices objectively from the vorticity [J]. *Journal of Fluid Mechanics*, 2016, 795: 136-173.
[21] Wang Y., Liu C. DNS study on bursting and intermittency in late boundary layer transition [J]. *Science China Physics, Mechanics and Astronomy*, 2017, 60(11): 114712.
[22] Golub G. H., Van Loan C. F. Matrix computation [M]. 4th Edition Baltimore, Maryland, USA: The Johns Hopkins University Press, 2013.
[23] Gallay T., Maekawa Y. Three-dimensional stability of burgers vortices [J]. *Communications in Mathematical Physics*, 2010, 302(2): 477-511.
[24] Haller G. An objective definition of a vortex [J]. *Journal of Fluid Mechanics*, 2005, 525: 1-26.
[25] Dong X., Yan Y., Yang Y. et al. Spectrum study on unsteadiness of shock wave–vortex ring interaction [J]. *Physics of Fluids*, 2018, 30(5): 056101.
[26] Gan Y., Liu J., Zhao N. et al. A numerical study on a Cartesian-based body-fitted adaptive grid method [J]. *International Journal of Computational Fluid Dynamics*, 2018, 32(4-5): 186-202.